© ARISER Vol. 5 No. 1 (2009) 31-40

Engineering: Re_En

Thermal Performance of Wire-Mesh Roughened Solar Air Heaters

M.K.PASWAN and S. P. SHARMA

Department of Mechanical Engineering, NIT, Jamshedpur, INDIA
{manikantp@yahoo.co.in sps_nitjsr2000@yahoo.co.in}

Received 14 December 2008; Accepted 27 December 2008

This paper presents an experimental study on thermal performance of five solar air heaters. All were providing wire-screen mesh (metal) as artificial roughened on the under side of its absorber plate. Instead of comparing the efficiency of the same rate of discharge, the same amount of pumping power was employed so that the unequal frictional losses were also taken into account in the comparison of overall heater efficiency. The rating parameters such as plate efficiency factor, heat-removal efficiency factor, over heat loss coefficient, and the effective absorption coefficient are reported for these heaters. The experiments were done at National Institute of Technology, Jamshedpur, India in the Thermal Engineering Laboratory. The Experimental study is reported for average winter conditions and the air heaters performance can be computed from these parameters for any other usual range of operating conditions.

Contents

1 Introduction

Solar Energy can be used for space heating, crop drying, timber seasoning and chicken breeding etc. The solar air heater is an attractive alternative energy source for the future at low and moderate temperature.

The use of artificial roughness on a surface is an effective technique to enhance the rate of heat transfer of fluid flowing in a duct. Turbulence promoted by roughness elements have been used to improve the convective heat transfer by creating turbulence in the flow. However, it would result in an increase in friction losses and hence, greater power requirement from a fan or blower. In order to keep the friction losses at minimum level, the turbulence must be created only in the region very close to the duct surface i.e. in laminar sub layer. The surface roughness can be produced by several methods, such as sand blasting, machining, casting, forming, welding ribs and by fixing thin circular wires along the surface. A number of investigations have been carried out on the heat transfer characteristics of channel or pipes with roughness elements on the surface. {Dippery & Sobersky [7]} developed a friction similarity law and a heat momentum transfer analogy for turbulent air flow in squire ducts with two opposite rib roughened walls. {Web & Eckert [6]} developed the heat transfer and friction factor correlation for turbulent air flow in tube having repeated rib number roughness. {Han & Zhang [5]} investigated the effect of broken rib orientation on local heat transfer distribution and pressure drop in square channels with two opposite ribbed walls. {Liou & Ho-Ming [?]} investigated experimentally the turbulent heat transfer and friction factor in channel wit ridges of various shapes mounted on two opposite walls.

Most of these investigations have been conducted for a turbine airfoil cooling design to optimize the ridge geometry in order to obtain the best heat transfer coefficients for either a given cooling flow rate on an available pressure drop across the cooling passage. It has recently been proposed by several investigators that the heat transfer capability of a solar air heater could be substantially enhanced by providing artificial roughness on the under side of its absorber plate. {Prasad & Malick [8]} utilized artificial roughness in a solar air heater in the form of small diameter wires to increase the heat transfer coefficients. {Prasad & saini [13, 16]} investigated fully developed turbulent flow in a solar air heater duct with a small diameter protrusion wire on the absorber plate. They investigated the heat transfer coefficient of solar air heaters, which can be increased by providing artificial roughness on the bottom of the absorber plate leading to higher thermal efficiency. They also determined the correlation between the optimization of the roughness and flow parameters (P/d, e/D, Re) to maximize that transfer while keeping friction losses minimum. {Sparrow & Tao [12]} investigated heat transfer and friction factor to evaluate the thermo hydraulic performance of unglazed solar air heaters having artificial roughness on the observer plate. {Gupta et al. [17, ?]} expressed heat and fluid flow in asymmetrically roughened rectangular ducts in transitionally rough flow to determine the effect of rib roughness on fluid flow and heat transfer in rectangular passages with only one heated surface having artificial rib roughness and flow in transitionally rough region. Correlations have been developed for transitionally rough flow in asymmetrically roughened rectangular ducts for geometrically dissimilar rib roughness height of 0.018 to 0.052. They also reported the effect of roughness and operating parameter on the thermal as well as hydraulic performance of roughened solar air heater and results are compared with conventional solar air heaters. The optimum design and operating conditions have also been investigated. A relationship between the system and operating parameters that combine to yield optimum performance has been developed. {Karwa et al. [?]} investigated that the heat transfer coefficient rectangular ducts, high range of parameter are Reynolds number from 3000 to 20000; relative roughness height from 0.141 to 0.328, the relative roughness pitch 4.5, 4.8, 7.0, and rib chamfer angles of -15, 0, 5, 10, 15, and 18; these correlation based on the low of wall similarity and heat momentum transfer analogy.

In the present paper, experimental investigations on wire mesh roughened absorber solar air heater of various geometrical parameters is being reported. The performance results are compared with those of plane collectors. Test is conducted under actual outdoor conditions for varying operating condition. These tests provide useful data for rating a solar air heater having its absorber artificially roughened with wire screen metal mesh.

2 Performance Equations

The heat transfer in a solar collector takes place by simultaneous conduction, convection, and radiation. The total useful energy collected per unit area is the difference between the amount of solar energy absorbed and the heat lost due to the collector being hotter than the surroundings. It is difficult to evaluate directly the rate of energy collection on an average daily or seasonal basis because of random fluctuation of weather. As such the heat transfer analysis is carried out on the assumption of instantaneous steady-state conditions. Through this analysis the performance characteristics or an air heater are correlated to the weather data, the design detail and operating condition of the air heater so as to yield a general functional relation between the large number of variables involved ay any instance.

The performance of a flat-plate collector operating under assumed steady-state conditions can be described by the following relationship

$$\frac{Q_u}{A_c} = l\,(\alpha\tau)\,e - U_L\,(\bar{t}_p - t_a) \tag{1}$$

$$\frac{Q_u}{A_c} = F_R\,(\alpha\tau)_e - F_R U_L\,(t_i - t_a) \tag{2}$$

Then the collector efficiency, η can be written from eqn. (1) or eqn. (2) as

$$\eta = (\alpha\tau)_e - U_L\left(\frac{t_p - t_a}{l}\right) \tag{3}$$

or

$$\eta = F_R\left[(\alpha\tau)_e - U_L\left(\frac{t_i - t_a}{l}\right)\right] \tag{4}$$

However, for solar air heaters taking in air at ambient temperature (t_0-t_a) it is advantageous to utilize the following equation for thermal efficiency.

$$\eta = F_0\left[(\alpha\tau)\,e - U_L\left(\frac{t_0 - t_a}{l}\right)\right] \tag{5}$$

where F_0 is the heat removal factor referred to the outlet temperature.

Eq. (5) indicates that a plot of efficiency against $[(t_0 - t_i)/l]$ will results in a straight line whose slope is F_0U_L and ordinate axis-intercept is $F_0(\tau\alpha)_c$ if F_0U_L and $(\tau\alpha)_c$ are not very strong functions of operating parameters like mass flow rate, intensity of solar radiations, ambient temperature and wind velocity variations. This approach, similar to the one conventionally used for solar flat-plate collectors, undoubtedly, assumes that the dependence of F_0 on mass flow rate which positively exists, is weak.

Furthermore, considering that the performance can be expressed by another equation, containing the temperature gain produced by the collector and expressed as

$$\eta = \frac{GC_p\,(t_0 - t_a)}{l} \tag{6}$$

Thus eqn. 5 and 6 can be represented on a single diagram having the same quantities as the abscissa and the ordinates {Sharma et al. [15]}. For a given collector, this diagram shows the typical performance parameters, η and $[(t_0 - t_i)/l]$ as a function of mass flow parameter G to represent eqn. (6) and as a single regression fit straight line plot to represent eqn. (5). This is considered to be the most appropriate representation of the thermal performance of solar air heater.

3 Experimental Set Up

Fig. 3 and 5 show the schematic diagram and photo of experimental set up and flow circuit two-dimensional flow was obtained by drawing atmospheric air through flow strengtheners (1). It is then passed through test section i.e., solar air heaters, one heater with wire screen roughened (3) and the other a plane (Flat-plate) collector (2). The test sections as shown in experimental setup consist of two rectangular channels of size 100x27x4 cm and glass cover at a height of 2 cm above the absorber. The bottom of the channel is insulated by 5 cm glass wool insulation supported on 5 mm plywood. The side middle of channels was of soft wood aving thickness of 25 mm and 30 mm respectively.

The flow straightner consisted of two symmetrical wooden rectangular duct 50x27x4 cm with bell-mounted entries. The will of ducts were similar in constructions to air heaters. The outlet of air heaters were connected through headers, orifice meter (5) and pipe fitting (4) to a centrifugal blower (7) coupled with 5-hp 3-phase electric motor as shown.

The assembly was mounted on wooden stands such that suction side of blower gets aligned with the axes of air heaters and flow straightners (1) in horizontal position. Mass flow rate of the air through wire-screen roughened collector (3) and plane collector (2) were measured by two orifice meter (5) which was fabricated as per standard specification. The flow rate is controlled by varying the speed of blower using pneumatic gun. Thermocouples (6) were used to measure the air and absorber plate temperature at different location. Solar radiation flux was recorded using a paranometer model No. 0052 supplied by National Instruments Ltd. Calcutta, India, having a constant of 129.31 watt per square m per mv.

4 Experimental Procedure

All the components of the set-up were checked for their position so that the collector covers and absorbers plate are in a horizontal position. The joints between the entry and exits sections of possible leakage were properly sealed. All the thermocouples were tested for their correctness while in site. Precaution was taken so that connector was not exposed to direct solar radiation which might lead to erroneous results. All other measuring instruments i.e., orifice meter, micro voltmeter and U tube manometer were properly checked.

Test runs were conducted under controlled condition for various mass flow rate and different type of wire screens (specifications given in Tab. 1 and Fig.2) under outdoor conditions with varying values of solar radiation intensity and ambient temperature. Test data were collected at hourly (half hourly in some cases) intervals each day between 9.00 AM to 2 P.M. in the month of Feb to May 2000. The following parameters were measured.

i) Pressure difference across orifice meter.
ii) Temperature of the absorber plate.
iii) Temperature of air in the duct.
iv) Ambient Temperature.
v) Intensity of solar radiation.

5 Results and Discussion

Figs. 1 and 4 show the experimental values of efficiencies of M-5 & M-1 as a function of the ratio of air temperature rise to isolation, i.e. $[(t_0 - t_i)/l]$ of plane and wire screen roughened absorber with varying physical characteristics i.e., for different wire diameter and mesh sizes of wire screens. Each line of these figures has been obtained from a firstorder least squares fit of the data for the particular physical parameters of absorber. These plots show that the efficiency of plane as well as wire screen roughened collector, increases with increase in mass flow rate and also with decreasing values of temperature rise parameters.

Comparison of the results of roughened collectors with those of planes collector show a substantial enhancement in efficiency as results of using wire screen roughened absorbers. It is seen in that efficiency of plane collectors increases from 28.5% to 30.7% as mass flow rate of air increases from increased from 0.003 kg/s-m^3 to 0.067 kg/s-m^2 and that of wire screen roughened absorber M_1 corresponding increase is from 46.3% to 51.2%. These values of efficiencies refer to regression lines where as the actual values have been found to very for each mass flow rate as the value of $[t_0 - t_i]$ varied at particular mass flow rate. Regression lines show an enhancement of efficiency of 20.5% at lowest mass flow rate (0.033 kg/s-m^2) and of 21.5% at highest mass flow rate (0.067 kg/s-m^2) mover plane collector for this wire screen roughened absorber (M_1)as shown in Fig. 4.

The value of efficiencies and corresponding enhancement of efficiency for several wire screen roughened and plane collectors at lowest and highest mass flow rates tested obtained from corresponding regression line are listed in Tab. 2. Inspection of this table shows that efficiency of plane collector increases with increases in mass flow rate and at fixed mass flow rate, there is slight variation in efficiency due to variations in isolation, ambient wind speed and sky-temperatures for all days of testing. It is also seen that the efficiency of wire-screen roughened absorber having pitch 1.814 mm (M_5) is greater than efficiency of 4.614 mm (M_1) for all values of mass flow rates.

Effects of geometric parameter of absorber on thermal performance of wire-screen roughened solar air heater were observed. The efficiency of plane solar air heater under similar operating condition was also shown in this Figure for compression. Performance lines are first-order least square fit (regression lines) of experimental data points, represented for respective values of geometric parameters of wire-screen roughened absorbers.

The difference in the performance of these roughened absorbers is due to difference in convective heat transfer coefficient between surface and flowing air roughness height and roughness pitch. It is seen that absorber with M_5 roughened surface exhibits over all best performance followed by collectors having M_4, M_3, M_2 and M_1 roughened absorber. This appears to the due to high value of convective heat transfer coefficient of absorber M_5 due to its lower value of pitch which creates more turbulence in the boundary sub layers. The absorber with high value of convective heat transfer coefficient transfer more energy to the flowing air causing resources plate temperature and consequently reduces the plate temperature and decreases heat losses, and increases the efficiency of this collector.

The value of performance parameter, $F_0(\tau\alpha)_c$, FU_L , F_0 and U_L obtained from intercept and slope of performance line are listed in Tab. 3. The value of F_0 have been calculated using a constant value of effective transmittance absorptance product of glass cover $(\tau\alpha)_c$ as 0.793 which is 1% greater than $(\tau\alpha)$ to include the effect of cover plate asborptance as suggested by {Whillier [**?**]}. The transmittance of glass of cover at normal incidence, $\tau = 0.827$ was used. The absorptance of absorbers with carbon black paint, $\alpha = 0.95$ has been sued. It is also possible to obtain the values of collector performance parameter $F_R(\tau\alpha)_c, F_RU_L$ and F_R from experimental values of slope (F_0F_L) and intercept $[F_0(\tau\alpha)_c]$ at any given mass flow rate. The values of parameters $F_R(\tau\alpha)_c$ and F_RU_L for these collectors as a functions of mass flow rate . The values of collector heat removal factor F_R , has been calculated using a constant of $(\tau\alpha)_c = 0.793$ as mentioned earlier. The values of F_R as a function of mass flow rate for this collector. A substantial enhancement of these parameters with geometrical parameter of roughness such as wire diameters, sizes of screen (pitches) is the index of the beneficial influence of providing wire screen roughness on the absorber plate of solar air heater.

6 Conclusion

1. Thermal performance of a solar air heater can be considerably enhanced by roughing the absorber plate with wire screen metal mesh and this enhancement is a strong function of geometrical parameter (such as diameter of wire, pitch) and operating parameters (viz. mass flow rate, insulation, inlet temperature).
2. Effect of parameters (diameter, pitch, isolation, inlet temperature and mass flow rates) on thermal performance has been investigated experimentally.
3. Decreasing values of wire-pitch leas to increasing value of thermal performance of solar air heater.

TAB. 1: Specification of Screen used given in Fig. 2

Type of Roughness Used	Mesh Per Inch	Wire Diameter (mm)	Transverse or Longitudinal Pitch (mm)	P/dc	Dc/Dn
M_1	5.5 x 5.5	0.508	4.614	6.05	37.24
M_2	8 x 8	0.508	3.175	4016	37.24
M_3	10 x 10	0.508	2.540	3.34	37.24
M_4	11.5 x 11.5	0.508	2.208	2.89	37.24
M_5	14 x 14	0.508	1.814	2.38	37.24

TAB. 2: Enhancement in efficiency

Fig. No.	Type of Roughness used	G. Kg/s-m^2	Efficiency of Plane Collector η_p (%)	Efficiency of Roughened Collector η_p (%)	Enhancement of Efficiency
Fig – 4	M_1	0.033	28.4	46.3	= 63.0%
		0.0667	30.7	51.2	= 72.1%
	M_2	0.033	28.6	48.1	= 69.3%
		0.0667	30.8	52.5	= 77.5%
	M_3	0.033	28.6	50.4	= 76.2%
		0.0667	30.8	54.1	= 76.4%
	M_4	0.033	28.3	51.8	= 83.0%
		0.0667	30.2	54.4	= 83.8%
Fig – 4	M_5	0.033	28.5	52.4	= 83.8%
		0.0667	30.2	56.3	= 86.4%

TAB. 3: Collector Performance Parameters

Type of Roughness	$F_0(\tau\alpha)_c$	F_0U_L	F_0	U_L
M_1	0.552	7.83	0.696	11.25
M_2	0.561	6.5	0.707	9.19
M_3	0.572	4.5	0.721	6.25
M_4	0.586	4.5	0.738	6.09
M_5	0.601	4.3	0.756	5.69
Plane	0.305	1.67	0.384	4.34

Nomenclature

A	heat transfer area, m^2
A_c	collector area, m^2
C_p	specific heat of air $J/kg°C$
d_e	diameter of wire, mm
F_0	heat removal factor related to outlet temperature
F_R	heat removal factor related to inlet temperature

G	air mass flow rate per unit collector area, Kg/s-m2
l	total solar energy incident upon plane of he collector per unit time per unit area W/m^2
P_t	transverse pitch representing center to center transverse distance between two consecutive wires, mm
P_L	longitudinal pitch representing center to center longitudinal distance between two consecutive wires, mm
Q_u	useful heat output, W
f_h	hydraulic radius, m
t_a	ambient air temperature, $^\circ C$
t_i	inlet temperature, $^\circ C$
t_0	outlet temperature, $^\circ C$
t_p	absorber surface temperature of the solar collector, $^\circ C$
η	Collector efficiency
$(\tau\alpha)_c$	effective transmittance- absorptance product for cover glass-absorber combination

References

1. Gupta, D., Solankin, S.C. & Saini, J.S. (1993) Heat and fluid flow in rectangular solar air heater ducts having transverse rib roughness on absorber plate. *Solar Energy,* **51**(1) 31-37.
2. Han, J.C. & Park, J.S. (1988) Developing heat transfer in rectangular channels with rib0turbulators. *It. J. Heat Mass Transfer,* **31**, 183-195.
3. Han, J.C., Glcksman, L.R. & Rohseneow W.M. (1978) An investigation of heat transfer and friction or rib-roughened surfaces. *Int. J. Heat Mass Transfer,* **21**, 1143-1156.
4. Han, J.C., Park, J.S. & Lei, C.K. (1989) Augmented heat transfer in rectangular channels of narrow aspect rations with rib turbulators. *Int. J. Heat Mass Transfer,* **32**, 1619-1630.
5. Han, J.C., Shang, Y.M. & Lee, C.P. (1991) Augmented heat transfer in square channel with parallel, crossed, and V-shaped angled ribs. *Journal of Heat Transfer,* **113**, 590-526.
6. Weeb, R.I., Eckert, E.R.G. & Goldstein, R.J. (1971) Heat transfer and friction in tubes with repeated rib-roughness. *Int. J. Heat Transfer,* **14**, 601-617.
7. Dippecy, D.F. & Saberskey, R.H. (1963) Heat and momentum transfer in smooth and rough tubes at various Prandti numbers. *Int. J. Heat Mass Transfer,* **6**, 239-253.
8. Prasad, K. & Mullick, S.C. (1989) Heat transfer characteristics of solar air heater used for drying purpose. *Applied Energy,* **13**, 83-93.
9. Cortes, A. & Piacemtini, R. (1990) Improvement of the efficiency of a bare Solar Collector by means of turbulence promoter. *Applied Energy,* **36**, 253-256.
10. Han, J.C., Park, J.S. & Lei, C.K. (1985) Heat transfer enhancement in channels with turbulence promoters. *Journal of Engineering for Gas Turbine & Power,* **107**, 628-635.
11. Vilemas, J.V. & Simonis, V.M. (1985) Heat transfer and friction of rough ducts carrying gas flow with variable physical properties. *Int. J. Heat Mass Transfer,* **28**, 59-68.
12. Sparrow, E.M. & Tao, W.Q. (1993) Enhanced heat transfer in a flat rectangular duct with stream wire period disturbances at one principal wall. *Journal of Heat Transfer,* **105**, 805-861.
13. Prasad, B.N. & Saini, J.S. (1988) Effect of artificial roughness on heat transfer and friction factor in a solar air heater. *Solar Energy,* **41**(6), 555-560.
14. Saini, R.P. & Saini, J.S. (1997) Heat transfer and friction factor correlations for artificially roughened duct with expanded metal as roughness elements. *Int. J. Heat Mass Transfer,* **40**(4), 973-986.
15. Sharma, S.P., Saini, J.S. & Verma, H.K. (1991) Thermal performance of packed-bed solar air heater. *Solar Energy,* **47**(2), 59-67.
16. Prasad, B.N. & Saini, J.S. (1991) Optimal thermohydraulic performance of artificially roughened solar air heater. *Solar Energy,* **47**(2), 91-96.
17. Gupta, D., Solanki, S.C. & Saini, J.S. (1997) Thermohydraulic performance of solar air heaters with roughened absorber plates. *Solar Energy,* **61**(1), 33-42.
18. Gupta, D., Solanki, S.C. & Saini, J.S. (1997) Heat and fluid flow in asymmetrically roughened rectangular ducts in transitionally rough flow. *Int. J. Energy, Heat & Mass Transfer,* **19**, 159-166.

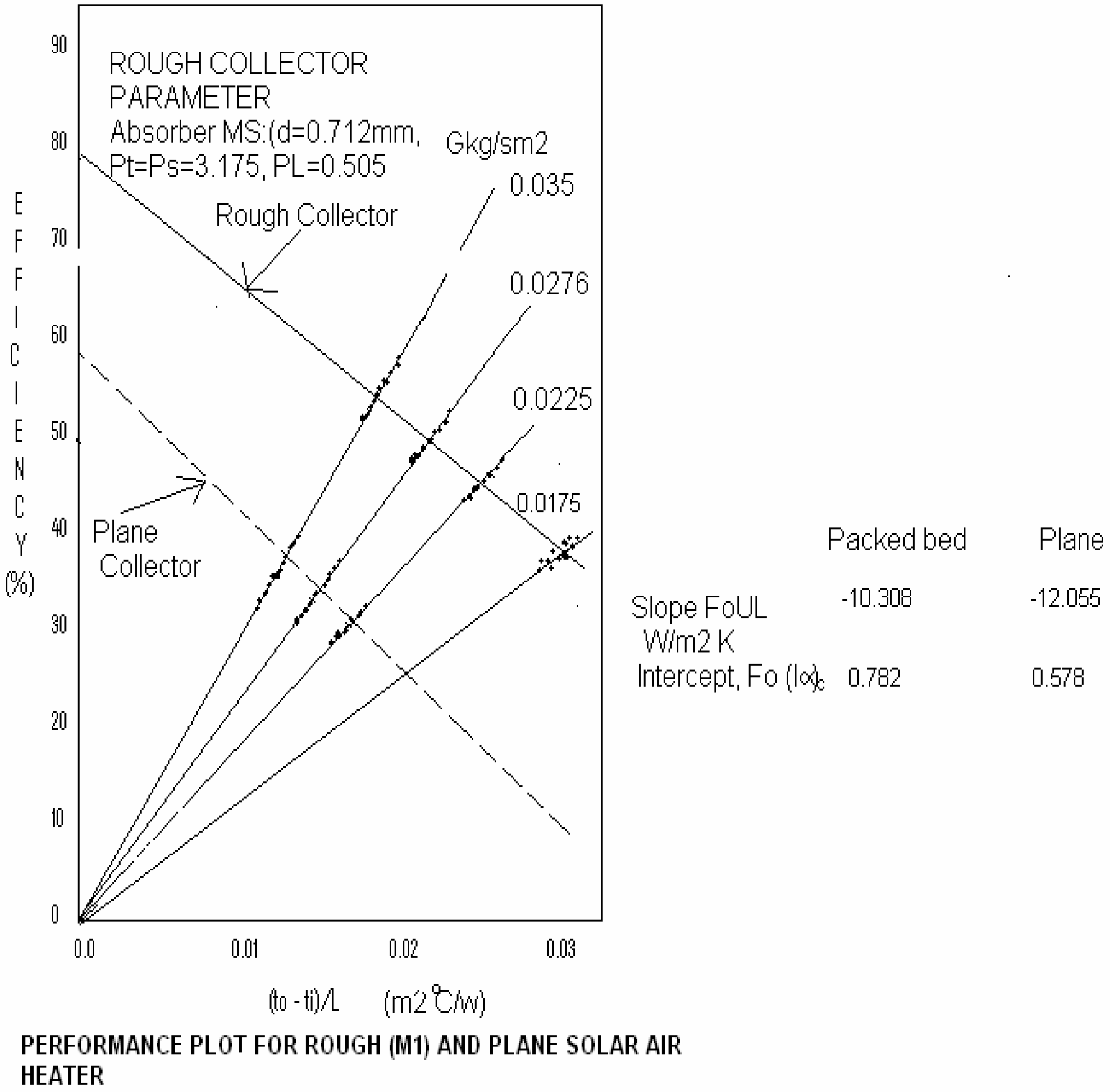

FIG. 1: Performance Plot.

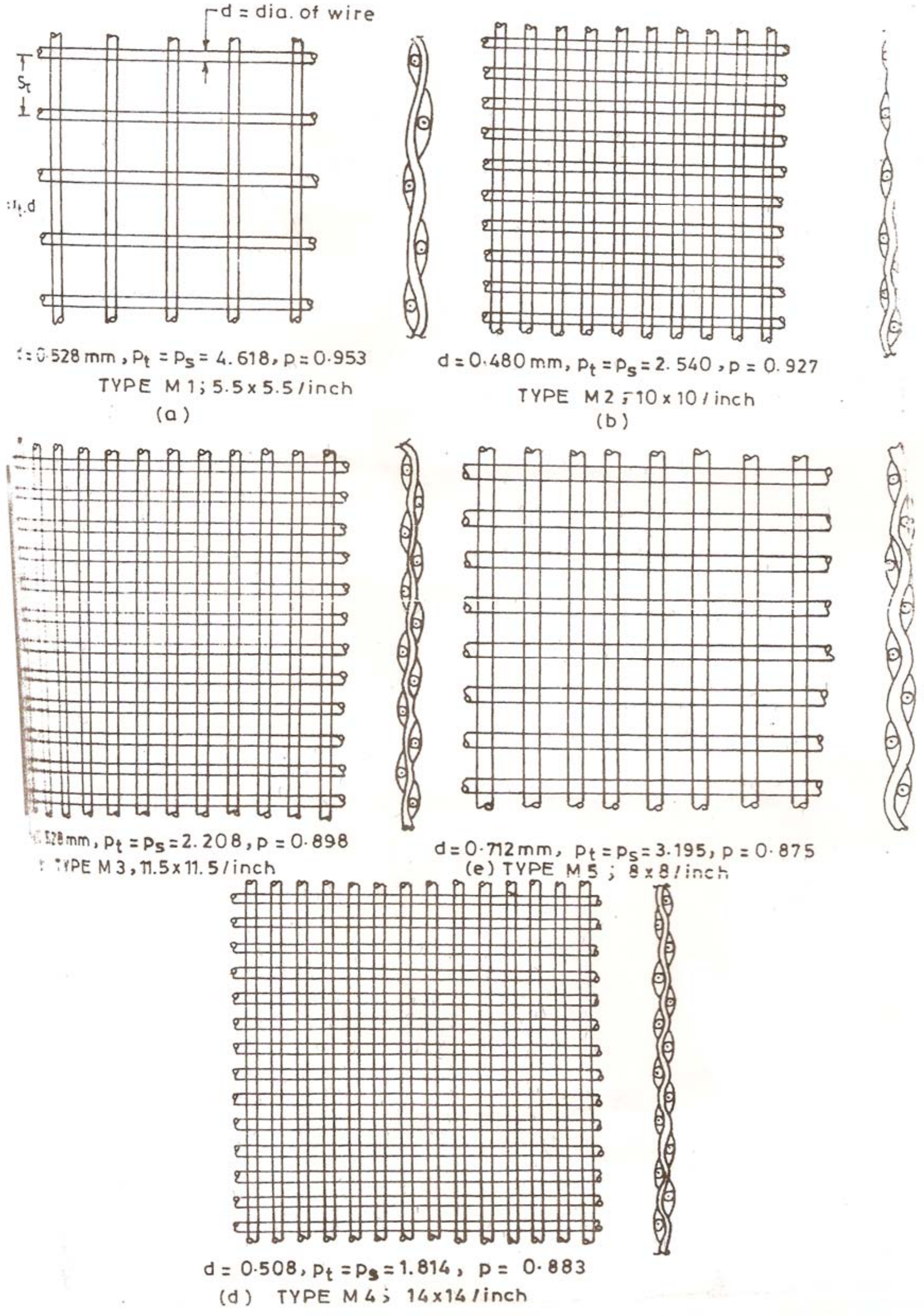

FIG. 2: All Type Of Absorber Plate.

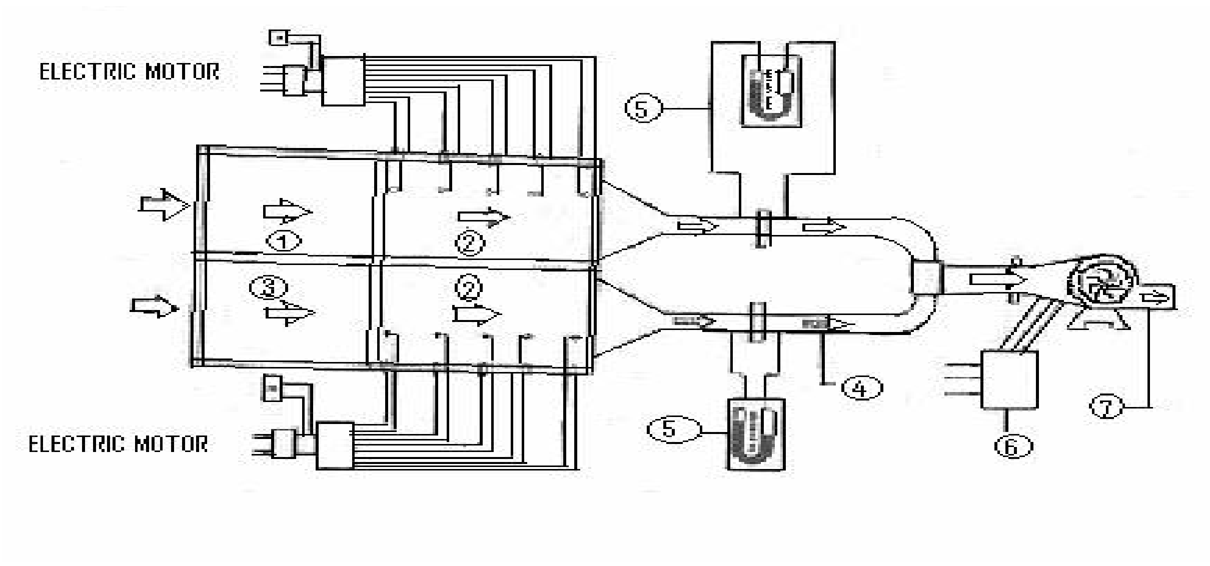

FIG. 3: Experimental Setup.

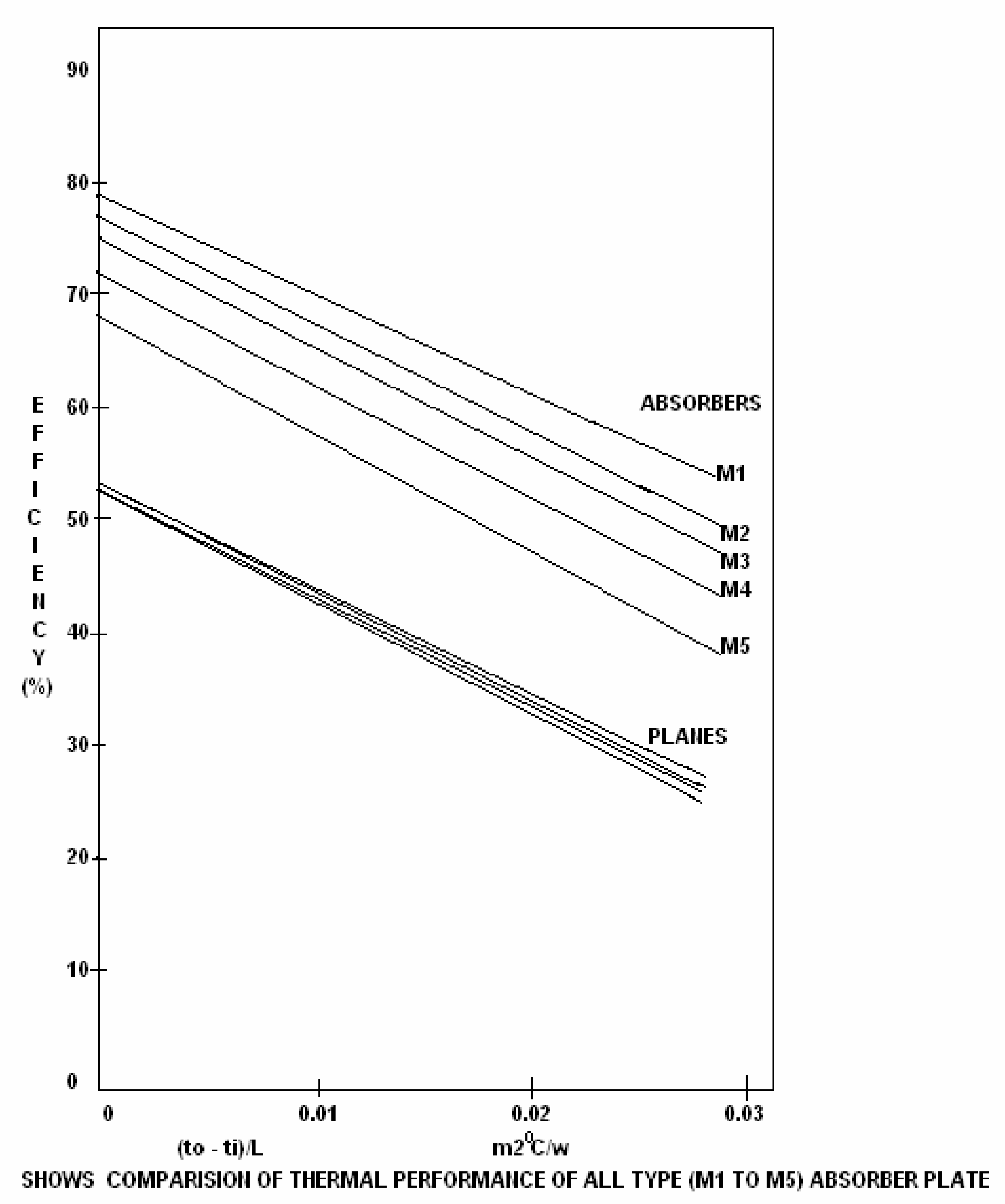

FIG. 4: Comparision Of Thermal Performanceof All Type (M-1 To M-5) Absorber Plate.

FIG. 5: Experimental Set Used As Solar Air Heater.